Commun. Comput. Phys.
doi: 10.4208/cicp.140813.230215a

Vol. **18**, No. 3, pp. 650-672
September 2015

A Finite Volume Scheme for Three-Dimensional Diffusion Equations

Xiang Lai[2], Zhiqiang Sheng[1] and Guangwei Yuan[1,*]

[1] *Laboratory of Science and Technology on Computational Physics, Institute of Applied Physics and Computational Mathematics, P.O. Box 8009, Beijing 100088, P.R. China.*
[2] *Department of Mathematics, Shandong University, Jinan 250100, P.R. China.*

Communicated by Chi-Wang Shu

Received 14 August 2013; Accepted (in revised version) 23 February 2015

Abstract. The extension of diamond scheme for diffusion equation to three dimensions is presented. The discrete normal flux is constructed by a linear combination of the directional flux along the line connecting cell-centers and the tangent flux along the cell-faces. In addition, it treats material discontinuities by a new iterative method. The stability and first-order convergence of the method is proved on distorted meshes. The numerical results illustrate that the method appears to be approximate second-order accuracy for solution.

AMS subject classifications: 65M08, 65M12, 65M55

Key words: Finite volume scheme, diffusion equation, tetrahedral meshes.

1 Introduction

Accurate and efficient discretization methods for the diffusion equation on distorted meshes are very important for the numerical simulations of Lagrangian hydrodynamics and magnetohydrodynamics. The finite volume method is widely used in solving these practical problems.

Many finite volume schemes for solving diffusion equations on non-rectangular meshes have been proposed. By using integral interpolation method, a nine point scheme for two-dimensional diffusion equation on arbitrary quadrilateral meshes is constructed in [1]. This scheme has only cell-centered unknowns after cell-vertex unknowns are eliminated by taking them as the arithmetic average of the neighboring cell-centered

*Corresponding author. *Email addresses:* qxlai2000@sdu.edu.cn (X. Lai), sheng_zhiqiang@iapcm.ac.cn (Z. Sheng), yuan_guangwei@iapcm.ac.cn (G. Yuan)

 ©2015 Global-Science Press

https://doi.org/10.4208/cicp.140813.230215a Published online by Cambridge University Press

unknowns. Numerical experiments show that it loses remarkably accuracy on moderately and highly skewed meshes. In [2] a continuous edge flux scheme for the stationary diffusion equation with smooth coefficient is proposed. The scheme in [3] needs both cell-centered unknowns and vertex unknowns on staggered meshes, and then a generalization of this scheme is proposed in [4] that can be applied to diffusion problems with discontinuous tensor coefficients. Later in [5], the convergence of the scheme of [3] is proved and the construction of the scheme is further extended to the diffusion problem with discontinuous coefficients on staggered meshes, moreover the discontinuity on cell edges is treated rigorously. The MDHW scheme in [6] rigorously treats material discontinuities and yields second-order accuracy regardless of the smoothness of the mesh. This scheme has face-centered unknowns in addition to cell-centered unknowns and the resulted matrix is asymmetric.

The support operators method (SOM) in [7–9] gives second-order accuracy on both smooth and non-smooth meshes either with or without material discontinuities, and SOM generally leads to a symmetric positive definite matrix. However, SOM has both cell-centered and face-centered unknowns or has a dense diffusion matrix, and there has no explicit discrete expression for the normal flux on a cell edge. The multipoint flux approximation (MPFA) method in [10–12] leads to a nonsymmetric matrix. It has only cell centered unknowns and gives an explicit expression for the face-centered flux. The flux is approximated by a multipoint flux expression based on transmissibility coefficients. These coefficients are computed by locally solving a small linear system.

Some successive works are devoted to the development of the schemes mentioned above. A similar finite volume scheme is proposed in [13] by using variation principle. To improve the accuracy, a method of eliminating vertex unknowns in the nine point scheme on distorted quadrilateral meshes is presented in [14], where the vertex unknowns are expressed as the interpolation of neighboring cell-centered unknowns based on certain rigorous derivation. The resulting scheme has only cell-centered unknowns and obtains second-order accuracy, however it leads to a nonsymmetric matrix in general. A different method of calculating the vertex unknowns of nine point scheme is proposed in [15], in which the vertex unknowns are solved independently on a new Voronoï mesh. This method is suitable for solving diffusion problems with discontinuous coefficients on highly distorted meshes and it is proved that this scheme has first-order convergence on distorted meshes.

Some finite volume schemes with full pressure support are presented in [16] and [17], where a method of M-matrix analysis is used to identify bounding limits for the scheme to posses a local discrete maximum principle and the conditions for the scheme to be positive definite are also derived. Based on SOM scheme, a mimetic finite difference method is proposed in [18, 19]. This method has been shown to be second-order accurate on non-smooth quadrilateral meshes with hanging nodes in both Cartesian and $r-z$ geometries.

For solving three-dimensional diffusion equation on distorted meshes, some cell-centered discrete schemes are discussed in [20]- [29]. Based on [1], a discrete scheme on the irregular hexahedral meshes is constructed in [20] by using integral interpolation

https://doi.org/10.4208/cicp.140813.230215a Published online by Cambridge University Press

method. In [21] and [22], the finite volume methods are developed for 3-D diffusion equation on nonorthogonal hexahedral and unstructured tetrahedral meshes, which can conserve the fluxes and is suitable for highly distorted meshes.

The scheme of [3,4], which is called DDFV (Discrete Duality Finite Volumes) scheme, is to integrate the equation over both a primal mesh and an associated dual mesh, and the unknowns are defined at both the cell-center and the cell-vertex, thus a large scale linear system is generated. Extensions of DDFV schemes to 3D [23–27] have two types (CV-DDFV and CeVeFE-DDFV). A feature of CV-DDFV scheme in [23] is the double covering of the domain by the dual mesh. CeVeFE-DDFV in [24, 25] contains cells, faces, edges and vertices unknowns. The scheme in [26] generally leads to non-symmetric matrices and it is not robust enough to handle certain types of highly distorted meshes or highly anisotropic diffusion tensors. The scheme in [27] leads to symmetric positive definite matrices and is more robust than that in [26]. However, it is limited to polyhedral cells whose faces have only three or four sides.

In [28], the method of [16] is extended to three-dimensional cases. The mimetic finite difference discretization of diffusion-type problems on unstructured polyhedral meshes is studied and extended to non-matching meshes in [29].

In this paper, we construct a cell-centered finite volume scheme for three-dimensional diffusion equation, where an intuitive derivation of discrete flux on mesh faces is given. Following the idea of [14], we eliminate the vertex unknowns for problems with continuous coefficient and prove that the method is stable and first-order convergence on distorted meshes. Moreover a new method of eliminating vertex unknowns on distorted meshes is presented to solve the discontinuous coefficient problems. The scheme leads to non-symmetric matrices and has a local stencil. But the matrix has excessive nonzero elements, so an iterative method is devised to solve the discrete system. Several numerical examples are given to illustrate the performance of the scheme.

The rest of this paper is organized as follows. In Section 2, we describe the construction of the finite volume scheme for stationary diffusion problems on distorted meshes and give the method to eliminate the vertex unknowns. In Section 3,we prove the stability and convergence of the scheme. In Section 4, we give the linear discrete system to be solved iteratively. In Section 5, some numerical experiments are presented to show how our scheme works for several test problems.

2 Construction of the scheme

2.1 Problem and notation

Consider the stationary diffusion problem with a Dirichlet boundary condition

$$-\nabla\cdot(\lambda(x)\nabla u)=f \quad \text{in } \Omega, \tag{2.1}$$

$$u(x)=g \quad \text{on } \partial\Omega, \tag{2.2}$$

https://doi.org/10.4208/cicp.140813.230215a Published online by Cambridge University Press

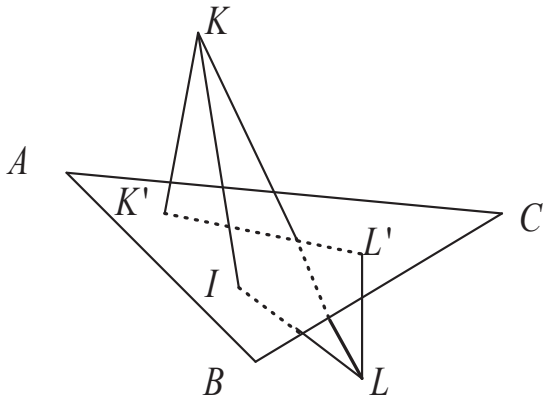


Figure 1: Stencil and notation.

where Ω is an open bounded set of R^3 with boundary $\partial\Omega$, and $\lambda=\lambda(x)$ is a scalar diffusion coefficient. Robin boundary condition will also be considered later.

In this paper, we use a mesh on Ω made up of tetrahedra and denote the neighboring cells by K and L. Let $\mathcal{J}$ be the set of all cells, $\mathcal{E}$ be the set of all cell faces, $\mathcal{E}_{int}$ be the set of all the cell faces not on $\partial\Omega$, and $\mathcal{E}_K$ be the set of all the cell face of cell K. Denote $h=\left(\sup_{K\in\mathcal{J}} m(K)\right)^{1/2}$, where $m(K)$ is the volume of cell K. With each cell K we associate one point denoted also by K: the barycenter is a qualified candidate but other points can also be chosen.

Denote the vertices by $A,B,C,D,\cdots$, and the cell face by S. $|S|$ is the area of S. If the cell face S is a common face of cells K and L, then denote $S=K|L$. Denote $\mathbf{n}_{KS}$ (resp. $\mathbf{n}_{LS}$) as the unit outer normal vector on the face S of cell K (resp. L). Then $\mathbf{n}_{KS}=-\mathbf{n}_{LS}$ holds for $S=K|L$.

The ray originated in the point K along $\mathbf{n}_{KS}$ intersects the plane that is generated by the cell face S, and the intersection point is denoted by K'. Similarly, the ray originated in the point L along $\mathbf{n}_{LS}$ intersects the plane generated by the cell face S, and the intersection point is L'. The point I is an arbitrary point on face S (see Fig. 1).

Define $u^-=u|_K, u^+=u|_L$, and similarly define λ^-,λ^+.

2.2 Construction of the scheme

From Fig. 1, we know that

$$\mathbf{n}_{KS}=\frac{\mathbf{KK'}}{|\mathbf{KK'}|},\quad \mathbf{n}_{LS}=\frac{\mathbf{LL'}}{|\mathbf{LL'}|}.$$

Since

$$\mathbf{KK'}=\mathbf{KI}+\mathbf{IK'},$$

we have

$$\nabla u^-(I)\cdot\mathbf{KK'}=\nabla u^-(I)\cdot\mathbf{KI}+\nabla u^-(I)\cdot\mathbf{IK'}.$$

https://doi.org/10.4208/cicp.140813.230215a Published online by Cambridge University Press

Then

$$\lambda^-\nabla u^-(I)\cdot\mathbf{n}_{KS}=\frac{\lambda^-}{|\mathbf{KK'}|}\nabla u^-(I)\cdot\mathbf{KI}+\frac{\lambda^-}{|\mathbf{KK'}|}\nabla u^-(I)\cdot\mathbf{IK'}$$
$$\approx\frac{\lambda^-}{|\mathbf{KK'}|}(u_I-u_K)+\frac{\lambda^-}{|\mathbf{KK'}|}\nabla u^-(I)\cdot\mathbf{IK'}. \tag{2.3}$$

Similarly, since

$$\mathbf{LL'}=\mathbf{IL'}+\mathbf{LI},$$

and

$$\nabla u^+(I)\cdot\mathbf{LL'}=\nabla u^+(I)\cdot\mathbf{IL'}+\nabla u^+(I)\cdot\mathbf{LI},$$

we have

$$\lambda^+\nabla u^+(I)\cdot\mathbf{n}_{LS}=\frac{\lambda^+}{|\mathbf{LL'}|}\nabla u^+(I)\cdot\mathbf{LI}+\frac{\lambda^+}{|\mathbf{LL'}|}\nabla u^+(I)\cdot\mathbf{IL'}$$
$$\approx\frac{\lambda^+}{|\mathbf{LL'}|}(u_I-u_L)+\frac{\lambda^+}{|\mathbf{LL'}|}\nabla u^+(I)\cdot\mathbf{IL'}. \tag{2.4}$$

From the continuity of the normal flux,

$$\lambda^-\nabla u^-(I)\cdot\mathbf{n}_{KS}=-\lambda^+\nabla u^+(I)\cdot\mathbf{n}_{LS},$$

there has

$$u_I=\frac{1}{a+b}\left[au_K+bu_L-b\nabla u^+\cdot\mathbf{IL'}-a\nabla u^-\cdot\mathbf{IK'}\right],$$

where $a=\frac{\lambda^-}{|\mathbf{KK'}|}$, $b=\frac{\lambda^+}{|\mathbf{LL'}|}$.

We know that the tangent derivative of u on S is continuous, i.e.,

$$\nabla u^-\cdot\mathbf{t}=\nabla u^+\cdot\mathbf{t},\ \ \forall\mathbf{t}\perp\mathbf{n}_{KS},\quad \text{on } S,$$

Denote $\nabla u\cdot\mathbf{t}=\nabla u^-\cdot\mathbf{t}=\nabla u^+\cdot\mathbf{t}$ on S, hence

$$\lambda^-\nabla u^-(I)\cdot\mathbf{n}_{KS}=a(u_I-u_K)+a\nabla u(I)\cdot\mathbf{IK'}$$
$$=\frac{ab}{a+b}[-u_K+u_L]+\nabla u\cdot\left[-\frac{ab}{a+b}\mathbf{IL'}+a\mathbf{IK'}-\frac{a^2}{a+b}\mathbf{IK'}\right]. \tag{2.5}$$

Moreover, from

$$\mathbf{IK'}=\mathbf{IL'}+\mathbf{L'K'},$$

then

$$\lambda^-\nabla u^-(I)\cdot\mathbf{n}_{KS}=\frac{ab}{a+b}\left[-u_K+u_L-\nabla u\cdot\mathbf{K'L'}\right].$$

Hence the discrete normal flux on S is

$$F_{K,S}=-\lambda^-\nabla u^-(I)\cdot\mathbf{n}_{KS}|S|=\frac{\lambda^+\lambda^-|S|}{\lambda^+|KK'|+\lambda^-|LL'|}\left[u_K-u_L+\nabla u\cdot\mathbf{K'L'}\right]. \tag{2.6}$$

https://doi.org/10.4208/cicp.140813.230215a Published online by Cambridge University Press

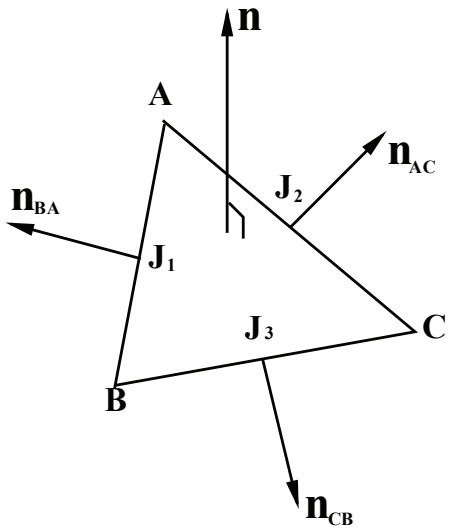


Figure 2: The face stencil.

Now we approximate ∇u on the face $S=\triangle ABC$ as follows.

$$\begin{aligned}\nabla u &= \frac{1}{|\triangle ABC|}\int_{\triangle ABC}\nabla u = \frac{1}{|\triangle ABC|}\int_{\partial\triangle ABC} u\mathbf{n}dl\\ &\approx \frac{1}{|\triangle ABC|}(u_{J_1}\mathbf{n}_{BA}+u_{J_2}\mathbf{n}_{AC}+u_{J_3}\mathbf{n}_{CB})\\ &\approx -\frac{1}{2|\triangle ABC|}(u_A\mathbf{n}_{CB}+u_B\mathbf{n}_{AC}+u_C\mathbf{n}_{BA}),\end{aligned} \tag{2.7}$$

where J_1, J_2 and J_3 are the midpoints of the edge BA, AC and CB respectively. Moreover the midpoints formulae, e.g., $u_{J_1}=\frac{1}{2}(u_A+u_B)$, have been used. And $\mathbf{n}_{AC}=\mathbf{n}\times\mathbf{AC}$,$\mathbf{n}_{BA}=\mathbf{n}\times\mathbf{BA}$, and $\mathbf{n}_{CB}=\mathbf{n}\times\mathbf{CB}$, and $\mathbf{n}$ is the unit normal vector to $\triangle ABC$ (see Fig. 2).

Substituting (2.7) into (2.6), we obtain

$$F_{K,S}=\frac{\lambda^-\lambda^+|S|}{\lambda^+|\mathbf{KK}'|+\lambda^-|\mathbf{LL}'|}\left[(u_K-u_L)-\frac{(u_A\mathbf{n}_{CB}+u_B\mathbf{n}_{AC}+u_C\mathbf{n}_{BA})\cdot\mathbf{K}'\mathbf{L}'}{2|S|}\right]. \tag{2.8}$$

Hence the finite volume scheme is constructed as follows:

$$\sum_{S\in\mathcal{E}_K}F_{K,S}=f_K m(K),\quad \forall K\in\mathcal{J}, \tag{2.9}$$

$$u_{Q_i}=g_{Q_i},\quad \forall Q_i\in\partial\Omega, \tag{2.10}$$

where $f_K=f(K), g_{Q_i}=g(Q_i)$.

https://doi.org/10.4208/cicp.140813.230215a Published online by Cambridge University Press

2.3 A general diffusion problem

In this subsection we consider a general diffusion problem with diffusion coefficient κ being a tensor.

We use the similar notations as above subsection. However here $\mathbf{KK}'$ means that the ray originated in the point K along the direction $\kappa^T\mathbf{n}_{KS}$ intersect the common face S and the intersection point is K'. Similarly, $\mathbf{LL}'$ means that the ray originated in the point L along the direction $\kappa^T\mathbf{n}_{LS}$ intersect the common face S and the intersection point is L'. $\mathbf{t}_{KK'}$ and $\mathbf{t}_{LL'}$ are the unit tangential vectors on the line KK' and LL', respectively.

Since

$$\begin{aligned}
&\nabla u^-(I)\cdot\mathbf{KK}'=\nabla u^-(I)\cdot\mathbf{KI}+\nabla u^-(I)\cdot\mathbf{IK}',\\
&\nabla u^+(I)\cdot\mathbf{LL}'=\nabla u^+(I)\cdot\mathbf{LI}+\nabla u^+(I)\cdot\mathbf{IL}',\\
&u_I-u_K\approx\nabla u^-(I)\cdot\mathbf{KI},\\
&u_I-u_L\approx\nabla u^+(I)\cdot\mathbf{LI},
\end{aligned}$$

one can obtain the following the discrete flux on S

$$\begin{aligned}
F_{K,S}&=-\nabla u^-\cdot\mathbf{t}_{KK'}\left|\kappa^T(K)\mathbf{n}_{KS}\right||S|\\
&=-\frac{\left|\kappa^T(K)\mathbf{n}_{KS}\right|}{|\mathbf{KK}'|}|S|\left(u_I-u_K+\nabla u^-\cdot\mathbf{IK}'\right), \qquad (2.11)\\
F_{L,S}&=-\nabla u^+\cdot\mathbf{t}_{LL'}\left|\kappa^T(L)\mathbf{n}_{LS}\right||S|\\
&=-\frac{\left|\kappa^T(L)\mathbf{n}_{LS}\right|}{|\mathbf{LL}'|}|S|\left(u_I-u_L+\nabla u^+\cdot\mathbf{IL}'\right). \qquad (2.12)
\end{aligned}$$

Similar to Section 2.2, from the continuity of the flux $F_{K,S}=-F_{L,S}$, we obtain

$$u_I=\frac{1}{a+b}\left[au_K+bu_L-(a+b)\nabla u\cdot\mathbf{IL}'-a\nabla u\cdot\mathbf{L}'\mathbf{K}'\right], \qquad (2.13)$$

here $a=\frac{\left|\kappa^T(K)\mathbf{n}_{KS}\right|}{|\mathbf{KK}'|}$, $b=\frac{\left|\kappa^T(L)\mathbf{n}_{LS}\right|}{|\mathbf{LL}'|}$.

From Eqs. (2.7), (2.11) and (2.13), we have

$$\begin{aligned}
F_{K,S}=\frac{\left|\kappa^T(K)\mathbf{n}_{KS}\right|\left|\kappa^T(L)\mathbf{n}_{LS}\right||S|}{\left|\kappa^T(K)\mathbf{n}_{KS}\right||\mathbf{LL}'|+\left|\kappa^T(L)\mathbf{n}_{LS}\right||\mathbf{KK}'|}&\left[(u_K-u_L)\right.\\
&\left.-\frac{1}{2|S|}(u_A\mathbf{n}_{CB}+u_B\mathbf{n}_{AC}+u_C\mathbf{n}_{BA})\cdot\mathbf{K}'\mathbf{L}'\right]. \qquad (2.14)
\end{aligned}$$

Thus the finite volume scheme for tensor diffusion problem is the same as (2.9)-(2.10) with discrete normal flux being replaced by (2.14).

https://doi.org/10.4208/cicp.140813.230215a Published online by Cambridge University Press

2.4 Robin boundary conditions

Consider the following Robin boundary conditions:

$$\alpha\kappa\nabla u\cdot\mathbf{v}+\beta u=g, \tag{2.15}$$

where $\mathbf{v}$ is the outward unit normal vector on the boundary $\partial\Omega$. Integrating (2.15) on cell-face $S\subset\partial\Omega$ leads to

$$\iint_S \alpha\kappa\nabla u\cdot\mathbf{v}+\iint_S \beta u=\iint_S g.$$

Now let K be the barycenter of S. Then

$$\alpha_K F_{K,S}+|S|\beta_K u_K=|S|g_K, \tag{2.16}$$

where the discrete flux $F_{K,S}$ is represented by (2.8) for scalar diffusion problems and by (2.14) for general tensor cases.

2.5 The approximation of cell vertex unknowns

From the above discussion, we know that the flux depends on the vertex unknowns in addition to cell-centered unknowns. It remains to consider how to eliminate the vertex unknowns locally, or approximate the vertex unknowns by certain combination of neighboring cell-centered unknowns. Compared with two-dimensional problem, it is more difficult to eliminate the vertex unknowns for the three-dimensional problem.

2.5.1 Continuous coefficient

For two-dimensional problems, a method to eliminate the vertex unknowns is proposed in [14]. That is, for a vertex Q, let $\mathcal{U}(Q)$ be the collection of all cells $K\in\mathcal{T}$ sharing Q as a vertex, and

$$u_Q=\sum_{K\in\mathcal{U}(Q)} u_K\omega_K. \tag{2.17}$$

The coefficients ω_K should satisfy the following relation:

$$\begin{cases} \sum\limits_{K\in\mathcal{U}(Q)}\omega_K=1, \\ \sum\limits_{K\in\mathcal{U}(Q)}\omega_K\mathbf{KQ}=\mathbf{0}. \end{cases} \tag{2.18}$$

The linear system (2.18) reduces to an under-determined system, and the least-square method is applied to solve it. The above interpolation technique can extent to three dimensional cases, but it is only suitable for continuous coefficient problems.

https://doi.org/10.4208/cicp.140813.230215a Published online by Cambridge University Press

2.5.2 Discontinuous coefficient

In [14] and [30], some methods were given to solve two-dimensional problem with discontinuous coefficient. However these methods can not directly extend to three-dimensional problems. In [28], each vertex unknown can be eliminated by solving a linear system. But this method is very expensive for three-dimensional problems. So a new efficient method should be proposed to eliminate the vertex unknowns for three-dimensional discontinuous problems.

In order to obtain the expression of the vertex unknown $u(Q)$, we firstly construct a control volume around vertex Q. Suppose that there are N tetrahedra surrounding a vertex Q. In each tetrahedron, we connect the midpoints A',B',C' of the three edges sharing Q, successively to obtain a tetrahedral region $QA'B'C'$, (see Fig. 3). Then the control volume of Q, denote as $Q^\star$, is formed. It is obvious that $Q^\star$ is a N-faced polyhedron.

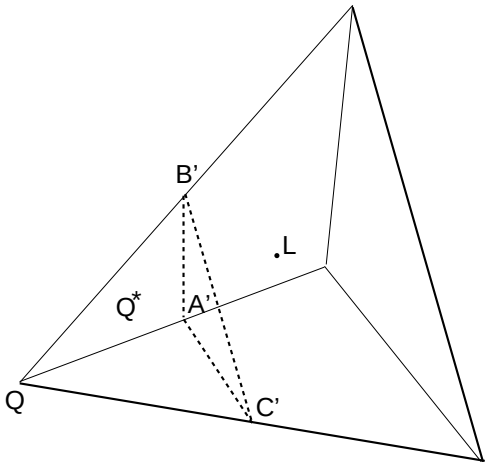


Figure 3: The control volume of vertex Q.

Similar to the process of Subsection 2.2, for cells $Q^\star$ and L, we can also construct the discrete normal flux $F_{Q,S'}$ on the surface S' of control volume $Q^\star$, that is

$$F_{Q,S'}=\frac{\lambda^-\lambda^+|S'|}{\lambda^+|\mathbf{QQ'}|+\lambda^-|\mathbf{LL'}|}\left[(u_Q-u_L)-\frac{(u_{A'}\mathbf{n}_{C'B'}+u_{B'}\mathbf{n}_{A'C'}+u_{C'}\mathbf{n}_{B'A'})\cdot\mathbf{Q'L'}}{2|S'|}\right].$$

In order to solve the vertex unknowns,we use iteration method to solve $u(Q)$. That is, the vertex unknowns of the $(s+1)$-th iterative step can be expressed by the linear combination of cell-centered unknowns and the midpoint unknowns of the s-th iterative step. The detailed method can be found in Section 4. Let $\mathcal{G}_Q$ be the set of all the cell-faces S' of $Q^\star$ and $\widetilde{\mathcal{J}}$ the set of all vertices. Then

$$\sum_{S'\in\mathcal{G}_Q}F_{Q,S'}=f(Q)m(Q),\quad\forall Q\in\widetilde{\mathcal{J}},\tag{2.19}$$

https://doi.org/10.4208/cicp.140813.230215a Published online by Cambridge University Press

where $m(Q)$ is the volume of $Q^\star$, and

$$F_{Q,S'}=\frac{\lambda^-\lambda^+|S'|}{\lambda^+|\mathbf{QQ'}|+\lambda^-|\mathbf{LL'}|}\left[(u_Q^{(s+1)}-u_L^{(s)})-\frac{(u_{A'}^{(s)}\mathbf{n}_{C'B'}+u_{B'}^{(s)}\mathbf{n}_{A'C'}+u_{C'}^{(s)}\mathbf{n}_{B'A'})\cdot\mathbf{Q'L'}}{2|S'|}\right], \tag{2.20}$$

where Q' and L' are the orthogonal projection of Q and L respectively onto the plane spanned by the triangle $A'B'C'$ as before. Note that here L is any cell with Q being a vertex. In Eq. (2.20), midpoint unknowns $u_{A'},u_{B'},u_{C'}$ can be expressed by the arithmetic average of corresponding vertex unknowns of s-th iterative step. This method can also deal with both continuous and discontinuous coefficient problems.

3 Stability and convergence of scheme

Suppose the vertex unknowns are eliminated by Eq. (2.17) and Eq. (2.18). Suppose the numbers of cells around vertex A,B,C are N_A,N_B,N_C respectively, then

$$u_A=\sum_{i=1}^{N_A}\omega_{A_i}u_{K_{A_i}},\quad u_B=\sum_{i=1}^{N_B}\omega_{B_i}u_{K_{B_i}},\quad u_C=\sum_{i=1}^{N_C}\omega_{C_i}u_{K_{C_i}},$$

where

$$\sum_{i=1}^{N_A}\omega_{A_i}=1,\quad \sum_{i=1}^{N_B}\omega_{B_i}=1,\quad \sum_{i=1}^{N_C}\omega_{C_i}=1.$$

In order to obtain the theorems of stability and convergence, we firstly introduce some notations. In Eq. (2.8), let

$$\tau_S=\frac{\lambda^-\lambda^+|S|}{\lambda^+|\mathbf{KK'}|+\lambda^-|\mathbf{LL'}|},\quad D_S=-\frac{1}{2|S|}.$$

Then

$$F_{K,S}=-\tau_S(u_L-u_K-D_S(\eta_A u_A+\eta_B u_B+\eta_C u_C)), \tag{3.1}$$

where $S=\Delta ABC$, and

$$\eta_A=\mathbf{n}_{CB}\cdot\mathbf{K'L'},\quad \eta_B=\mathbf{n}_{AC}\cdot\mathbf{K'L'},\quad \eta_C=\mathbf{n}_{BA}\cdot\mathbf{K'L'},$$

and there holds $\eta_A+\eta_B+\eta_C=0$. The following three assumptions will be needed.

Assumption (H1): $u(x)\in C^2(K),\lambda(x)\in C^1(K)$ and $f(x)\in C^1(K)$ for all $K\in\mathcal{J}$; and $g(x)\equiv 0$ on $\partial\Omega$.

Denote $\mathcal{E}_S$ be the set of all the cell faces neighboring to the cell face S. That is, the cell faces in $\mathcal{E}_S$ has at least a common vertex with S. Let $N_{S'}$ be the number of cell neighboring to cell face S', where $S'\in\mathcal{E}_S$.

https://doi.org/10.4208/cicp.140813.230215a Published online by Cambridge University Press

Assumption (H2): for each cell face S

$$\tau_S D_S^2 \omega_{S'}^2 \leq \frac{1-\varepsilon}{N_{S'}^2}\tau_{S'},$$

where $\varepsilon>0$ is a given small constant, and $\omega_{S'}$ will be defined in the following subsection.

Assumption (H3): For a mesh $\mathcal{J}$ on Ω, there is a constant $C>0$ such that the following discrete Poincare inequality holds for any discrete function $\{u_K|K\in\mathcal{J}\bigcup(\mathcal{E}\bigcap\partial\Omega)\}$ satisfying $u_K=0$ for all $K\in\mathcal{E}\bigcap\partial\Omega$,

$$\sum_{K\in\mathcal{J}}|u_K|^2 m(K)\leq C\sum_{S\in\mathcal{E}_{int}}\tau_S(u_L-u_K)^2.$$

Remark 3.1. For the discrete Poincare inequality we refer to [31] and [32].

3.1 Stability

Now we prove that our scheme is stable.

Theorem 3.1. *Assume* (H1), (H2) *are satisfied. Then there exists a constant C, independent of h, such that,*

$$\sum_{S\in\mathcal{E}}\tau_S(u_L-u_K)^2\leq C\sum_{K\in\mathcal{J}}|f_K|^2 m(K).$$

Proof. Multiplying Eq. (2.9) by u_K, and summing up the resulting products for $K\in\mathcal{J}$, we get

$$\sum_{K\in\mathcal{J}}\sum_{S\in\mathcal{E}_K}F_{K,S}u_K=\sum_{K\in\mathcal{J}}f_K u_K m(K). \tag{3.2}$$

Notice that

$$\begin{aligned}
\sum_{K\in\mathcal{J}}\sum_{S\in\mathcal{E}_K}F_{K,S}u_K &= -\sum_{K\in\mathcal{J}}\sum_{S\in\mathcal{E}_K}\tau_S(u_L-u_K-D_S(\eta_A u_A+\eta_B u_B+\eta_C u_C))u_K\\
&=\sum_{S\in\mathcal{E}}\tau_S(u_L-u_K)^2+\sum_{S\in\mathcal{E}_{int}}\tau_S D_S(\eta_A u_A+\eta_B u_B+\eta_C u_C)(u_K-u_L)\\
&=\sum_{S\in\mathcal{E}}\tau_S(u_L-u_K)^2+\sum_{S\in\mathcal{E}_{int}}\tau_S D_S(\eta_A(u_A-u_C)+\eta_B(u_B-u_C))(u_K-u_L)\\
&=\sum_{S\in\mathcal{E}}\tau_S(u_L-u_K)^2+\sum_{S\in\mathcal{E}_{int}}\tau_S D_S\Big(\eta_A\Big(\sum_{i=1}^{N_A}\omega_{A_i}u_{K_{A_i}}-\sum_{i=1}^{N_C}\omega_{C_i}u_{K_{C_i}}\Big)\\
&\quad+\eta_B\Big(\sum_{i=1}^{N_B}\omega_{B_i}u_{K_{B_i}}-\sum_{i=1}^{N_C}\omega_{C_i}u_{K_{C_i}}\Big)\Big)(u_K-u_L)\\
&=\sum_{S\in\mathcal{E}}\tau_S(u_L-u_K)^2+\sum_{S\in\mathcal{E}_{int}}\tau_S D_S\sum_{S'\in\mathcal{E}_S}\omega_{S'}(u_{S',1}-u_{S',2})(u_K-u_L),
\end{aligned}\tag{3.3}$$

https://doi.org/10.4208/cicp.140813.230215a Published online by Cambridge University Press

where $\omega_{S'}$ is defined such that

$$\eta_A\Big(\sum_{i=1}^{N_A}\omega_{A_i}u_{K_{A_i}}-\sum_{i=1}^{N_C}\omega_{C_i}u_{K_{C_i}}\Big)+\eta_B\Big(\sum_{i=1}^{N_B}\omega_{B_i}u_{K_{B_i}}-\sum_{i=1}^{N_C}\omega_{C_i}u_{K_{C_i}}\Big)=\sum_{S'\in\mathcal{E}_S}\omega_{S'}(u_{S',1}-u_{S',2}),$$

and $u_{S',1}$ and $u_{S',2}$ are two cell-centered unknowns which are defined in the center of two cells sharing the cell face S'.

Substitute Eq. (3.3) into Eq. (3.2) to obtain

$$\sum_{S\in\mathcal{E}}\tau_S(u_L-u_K)^2+\sum_{S\in\mathcal{E}_{int}}\tau_S D_S\sum_{S'\in\mathcal{E}_S}\omega_{S'}(u_{S',1}-u_{S',2})(u_K-u_L)=\sum_{K\in\mathcal{J}}f_K u_K m(K).$$

By the Cauchy inequality,

$$\begin{aligned}\sum_{S\in\mathcal{E}}\tau_S(u_L-u_K)^2\le&\sum_{S\in\mathcal{E}_{int}}\sum_{S'\in\mathcal{E}_S}\frac{\tau_S}{2N_{S'}}(u_L-u_K)^2+\sum_{S\in\mathcal{E}_{int}}\sum_{S'\in\mathcal{E}_S}\frac{N_{S'}\tau_S}{2}D_S^2\omega_{S'}^2(u_{S',1}-u_{S',2})^2\\&+\frac{C}{\varepsilon}\sum_{K\in\mathcal{J}}|f_K|^2m(K)+\frac{\varepsilon}{4C}\sum_{K\in\mathcal{J}}|u_K|^2m(K).\end{aligned}$$

Apply the assumptions (H2) and (H3) to obtain

$$\begin{aligned}\sum_{S\in\mathcal{E}}\tau_S(u_L-u_K)^2\le&\sum_{S\in\mathcal{E}_{int}}\frac{1}{2}\tau_S(u_L-u_K)^2+\sum_{S\in\mathcal{E}_{int}}\sum_{S'\in\mathcal{E}_S}\frac{1-\varepsilon}{2N_{S'}}\tau_{S'}(u_{S',1}-u_{S',2})^2\\&+\frac{C}{\varepsilon}\sum_{K\in\mathcal{J}}|f_K|^2m(K)+\frac{\varepsilon}{4C}\sum_{K\in\mathcal{J}}|u_K|^2m(K)\\\le&\sum_{S\in\mathcal{E}_{int}}\frac{1}{2}\tau_S(u_L-u_K)^2+\sum_{S\in\mathcal{E}_{int}}\frac{1-\varepsilon}{2}\tau_S(u_L-u_K)^2\\&+\frac{C}{\varepsilon}\sum_{K\in\mathcal{J}}|f_K|^2m(K)+\frac{\varepsilon}{4}\sum_{S\in\mathcal{E}_{int}}\tau_S(u_L-u_K)^2,\end{aligned}$$

which follows

$$\sum_{S\in\mathcal{E}}\frac{\varepsilon}{4}\tau_S(u_L-u_K)^2\le\frac{C}{\varepsilon}\sum_{K\in\mathcal{J}}|f_K|^2m(K),$$

hence,

$$\sum_{S\in\mathcal{E}}\tau_S(u_L-u_K)^2\le C\sum_{K\in\mathcal{J}}|f_K|^2m(K).$$

So the scheme (2.9)-(2.10) is proved to be stable. □

https://doi.org/10.4208/cicp.140813.230215a Published online by Cambridge University Press

3.2 Convergence

By integrating Eq. (2.1) over the cell K and using the Green formula, one obtains

$$\sum_{S\in\mathcal{E}_K}\mathcal{F}_{K,S}=\int_K f(x)dx, \tag{3.4}$$

where $\mathcal{F}_{K,S}$ is the normal face flux on the edge S, and it is defined by

$$\mathcal{F}_{K,S}=-\int_S \lambda(x)\nabla u(x)\cdot\mathbf{n}_{K,S}dl, \tag{3.5}$$

with $\mathbf{n}_{K,S}$ the outward unit normal on the edge S of cell K. Eq. (3.4) is equivalent to the following equation:

$$\sum_{S\in\mathcal{E}_K}\mathcal{F}_{K,S}=f_K m(K)+S_K m(K), \tag{3.6}$$

where $f_K=f(K)$,$S_K=\int_K(f(x)-f_K)dx/m(K)$. Obviously, $|S_K|\le Ch$ by the assumption (H1).

From Eq. (3.5), we have

$$\mathcal{F}_{K,S}=-\tau_S(u(L)-u(K)-D_S(\eta_A u(A)+\eta_B u(B)+\eta_C u(C)))+W_{K,S}, \tag{3.7}$$

where $W_{K,S}=\mathcal{O}(h^2)$. Denote

$$\tilde{F}_{K,S}=-\tau_S(u(L)-u(K)-D_S(\eta_A u(A)+\eta_B u(B)+\eta_C u(C))), \tag{3.8}$$

then

$$\mathcal{F}_{K,S}=\tilde{F}_{K,S}+W_{K,S}.$$

Let $e_K=u(K)-u_K$, subtract (2.9) from (3.6) to obtain

$$\sum_{S\in\mathcal{E}_K}G_{K,S}=S_K m(K)-\sum_{S\in\mathcal{E}_K}W_{K,S}, \tag{3.9}$$

where $G_{K,S}=\tilde{F}_{K,S}-F_{K,S}$.

Now we present an error estimate for the scheme (2.9)-(2.10).

Theorem 3.2. *Assume* (H1), (H2) *and* (H3) *are satisfied. Then there exists a constant C, independent of h, such that,*

$$\left(\sum_{S\in\mathcal{E}}\tau_S(e_L-e_K)^2\right)^{1/2}\le Ch.$$

Proof. Multiplying (3.9) by e_K, and summing up the resulting products for $K\in\mathcal{J}$, we get

$$\sum_{K\in\mathcal{J}}\sum_{S\in\mathcal{E}_K}G_{K,S}e_K=\sum_{K\in\mathcal{J}}S_K e_K m(K)-\sum_{K\in\mathcal{J}}\sum_{S\in\mathcal{E}_K}W_{K,S}e_K. \tag{3.10}$$

https://doi.org/10.4208/cicp.140813.230215a Published online by Cambridge University Press

Notice that

$$\begin{aligned}
&\sum_{K\in\mathcal{J}}\sum_{S\in\mathcal{E}_K} G_{K,S}e_K \\
&=-\sum_{K\in\mathcal{J}}\sum_{S\in\mathcal{E}_K}\tau_S\Big(e_L-e_K-D_S\Big(\eta_A\sum_{i=1}^{N_A}\omega_{A_i}e_{K_{A_i}}+\eta_B\sum_{i=1}^{N_B}\omega_{B_i}e_{K_{B_i}}+\eta_C\sum_{i=1}^{N_C}\omega_{C_i}e_{K_{C_i}}\Big)\Big)e_K \\
&=\sum_{S\in\mathcal{E}}\tau_S(e_L-e_K)^2+\sum_{S\in\mathcal{E}_{int}}\tau_S D_S\Big(\eta_A\sum_{i=1}^{N_A}\omega_{A_i}e_{K_{A_i}}+\eta_B\sum_{i=1}^{N_B}\omega_{B_i}e_{K_{B_i}}+\eta_C\sum_{i=1}^{N_C}\omega_{C_i}e_{K_{C_i}}\Big)(e_K-e_L).
\end{aligned} \tag{3.11}$$

Denote $W_S=W_{K,S}$, notice $W_{L,S}=-W_{K,S}$, and substitute Eq. (3.11) into Eq. (3.10). Similar to the proof of stability, we can obtain

$$\sum_{S\in\mathcal{E}}\tau_S(e_L-e_K)^2\le Ch^2.$$

The proof of Theorem 3.2 is finished. □

4 Discrete system

Substituting Eq. (2.8) into Eq. (2.9), we obtain a nonsymmetric algebraic system:

$$AU=F, \tag{4.1}$$

where U is the vector of cell-centered unknowns. The system (4.1) may be solved by a number of different method. When we use (2.17), (2.18) to eliminate the vertex unknowns, for the small mesh size, the matrix A has excessive nonzero elements so it is difficult to solve the system (4.1) by usual iterative methods. So we use (2.19)-(2.20) to eliminate the vertex unknowns. Rewrite Eq. (4.1) as:

$$BU=\bar{F}, \tag{4.2}$$

where $B=\sum_{S\in\mathcal{E}}N_S B_S N_S^T$ is represented by assembling of 2×2 matrices

$$B_S=\begin{pmatrix} \frac{\lambda^-\lambda^+|S|}{\lambda^+|\mathbf{KK'}|+\lambda^-|\mathbf{LL'}|} & -\frac{\lambda^-\lambda^+|S|}{\lambda^+|\mathbf{KK'}|+\lambda^-|\mathbf{LL'}|} \\ -\frac{\lambda^-\lambda^+|S|}{\lambda^+|\mathbf{KK'}|+\lambda^-|\mathbf{LL'}|} & \frac{\lambda^-\lambda^+|S|}{\lambda^+|\mathbf{KK'}|+\lambda^-|\mathbf{LL'}|} \end{pmatrix}$$

for interior faces and 1×1 matrices $B_S=\frac{\lambda^-\lambda^+|S|}{\lambda^+|\mathbf{KK'}|+\lambda^-|\mathbf{LL'}|}$ for boundary faces. N_S are assembling matrices consisting of zeros and ones. And each component in the term $\bar{F}$ at the right of Eq. (4.2) for each $K\in\mathcal{J}$ is:

$$f_K m(K)+\sum_{S\in\mathcal{E}_K}\frac{\lambda^-\lambda^+}{2(\lambda^+|\mathbf{KK'}|+\lambda^-|\mathbf{LL'}|)}(u_A\mathbf{n}_{CB}+u_B\mathbf{n}_{AC}+u_C\mathbf{n}_{BA})\cdot\mathbf{K'L'}. \tag{4.3}$$

https://doi.org/10.4208/cicp.140813.230215a Published online by Cambridge University Press

The right term $\bar{F}$ contains the values of the vertex unknowns, and then the number of the nonzero elements of the matrix B is remarkably less than that of the matrix A. Thus we use the following iteration method to solve system (4.2): Choose a small value $\varepsilon_{non}>0$, initial cell-centered vector $U^0\geq 0$ and initial vertices vector $V^0\geq 0$, and repeat for the iterative index $s=1,2,\cdots$,

1. Using Eq. (2.19), Eq. (2.20) and U^{s-1},V^{s-1} to calculate the vertex unknowns V^s. Then $\bar{F}^s$ is obtained by Eq. (4.3).

2. Solve $BU^s=\bar{F}^s$.

3. Using Eq. (2.19), Eq. (2.20) and U^s,V^s to calculate V^{s+1}. And $\bar{F}^{s+1}$ is obtained.

4. Repeat steps 2 and 3 if $\left\|BU^s-\bar{F}^{s+1}\right\|>\varepsilon_{non}\left\|BU^0-\bar{F}^0\right\|$.

The linear system (4.2) with non-symmetric matrix B is solved by GMRES method. The GMRES iterations are terminated when the relative norm of the initial residual becomes smaller than ε_{lin}. In our numerical experiments, we take $\varepsilon_{non}=1.0e^{-7},\varepsilon_{lin}=1.0e^{-8}$, and we gave the number of iteration.

5 Numerical examples

The discrete L_2-norms is used to evaluate approximation errors. For the solution u, the following L_2-norm is applied:

$$\varepsilon_2^u=\left[\sum_{K\in\mathcal{J}}(u_K-u(K))^2m(K)\right]^{\frac{1}{2}}.$$

We use two mesh partitions: the uniform and random tetrahedral meshes. To construct such a mesh, we take a uniform cubic partition on $\Omega=[0,1]^3$ with a mesh size h, and divide each cube into 24 uniform tetrahedra or 24 random tetrahedra with randomly distorted position of mesh nodes:

$$\begin{aligned}X&=x+\xi_x h,\\ Y&=y+\xi_y h,\\ Z&=z+\xi_z h,\end{aligned}$$

where ξ_x, ξ_y and ξ_z are random variables with values between -0.3 and 0.3. Fig. 4 gives an example of distorted tetrahedral meshes ($h=1/8$).

https://doi.org/10.4208/cicp.140813.230215a Published online by Cambridge University Press

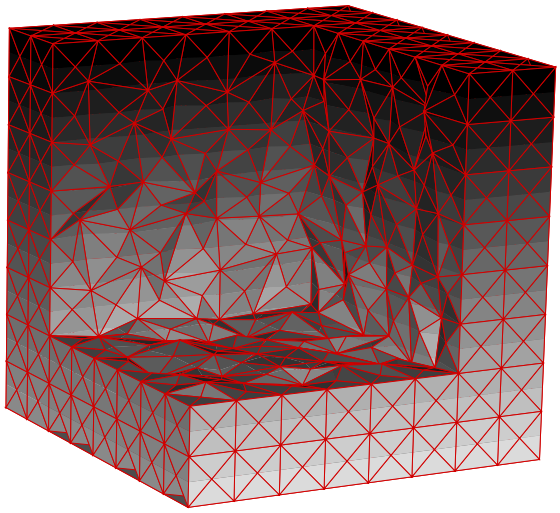


Figure 4: An example of a random tetrahedral meshes ($h=1/8$).

5.1 Scalar diffusion coefficient

Consider the problem (2.1)-(2.2) with Dirichlet boundary condition in the unit cube $\Omega=[0,1]^3$.

Let $\lambda(x,y,z)=1+x+y+z$. The exact solution is chosen to be

$$u=\sin(\pi x)\sin(\pi y)\sin(\pi z).$$

Then the corresponding source function

$$\begin{aligned} f=&3\pi^2\lambda(x,y,z)\sin(\pi x)\sin(\pi y)\sin(\pi z)-\pi(\cos(\pi x)\sin(\pi y)\sin(\pi z)\\ &+\sin(\pi x)\cos(\pi y)\sin(\pi z)+\sin(\pi x)\sin(\pi y)\cos(\pi z)), \end{aligned}$$

and the boundary condition is $g=0$.

Tables 1 and 2 give the L_2-norm of errors between exact solutions and numerical solutions, respectively. From Table 1, one can see that the method is second order convergence for the solution on uniform tetrahedral meshes. From Table 2, one can see that, on random tetrahedral meshes, the convergent order for the solution is almost second order.

5.2 Full anisotropic tensor (Dirichlet boundary condition)

Consider the general problem (2.3) with Dirichlet boundary condition in the unit cube $\Omega=[0,1]^3$.

Let κ be the symmetric positive definite matrix defined by

$$\kappa=\begin{pmatrix} \cos\theta & -\sin\theta & 0\\ \sin\theta & \cos\theta & 0\\ 0 & 0 & 1 \end{pmatrix}\begin{pmatrix} 1 & 0 & 0\\ 0 & \varepsilon & 0\\ 0 & 0 & \eta(1+x+y+z) \end{pmatrix}\begin{pmatrix} \cos\theta & \sin\theta & 0\\ -\sin\theta & \cos\theta & 0\\ 0 & 0 & 1 \end{pmatrix},$$

https://doi.org/10.4208/cicp.140813.230215a Published online by Cambridge University Press

Table 1: Numerical results for scalar diffusion coefficient on uniform tetrahedral meshes.

The number of cell	24×4^3	24×8^3	24×16^3	24×32^3	24×64^3
Mesh size (h)	1/4	1/8	1/16	1/32	1/64
ε_2^u	4.93e-3	1.10e-3	2.65e-4	6.55e-5	1.63e-5
Rate	·····	2.16	2.05	2.02	2.01
The number of iteration	8	7	6	5	4

Table 2: Numerical results for scalar diffusion coefficient on distorted tetrahedral meshes.

The number of cell	24×4^3	24×8^3	24×16^3	24×32^3	24×64^3
Mesh size (h)	1/4	1/8	1/16	1/32	1/64
ε_2^u	1.72e-2	3.25e-3	8.29e-4	2.03e-4	5.01e-5
Rate	·····	2.40	1.97	2.03	2.02
The number of iteration	9	9	9	10	10

Table 3: Numerical results for full anisotropic tensor on uniform tetrahedral meshes.

The number of cell	24×4^3	24×8^3	24×16^3	24×32^3	24×64^3
Mesh size (h)	1/4	1/8	1/16	1/32	1/64
ε_2^u	2.36e-2	5.91e-3	1.47e-3	3.67e-4	9.18e-5
Rate	·····	2.00	2.00	2.00	2.00
The number of iteration	26	35	40	41	40

Table 4: Numerical results for full anisotropic tensor on distorted tetrahedral meshes.

The number of cell	24×4^3	24×8^3	24×16^3	24×32^3	24×64^3
Mesh size (h)	1/4	1/8	1/16	1/32	1/64
ε_2^u	3.27e-2	8.03e-3	2.23e-3	5.86e-4	1.49e-4
Rate	·····	2.02	1.85	1.93	1.98
The number of iteration	27	60	75	87	103

where $\theta=\frac{\pi}{6}$, $\varepsilon=0.1$, $\eta=10$. The exact solution is chosen to be $u=\sin(\pi x)\sin(\pi y)\sin(\pi z)$, and the corresponding source function is

$$\begin{aligned} f=&\pi^2(1+\varepsilon+\eta(1+x+y+z))\sin(\pi x)\sin(\pi y)\sin(\pi z)\\ &-2(1-\varepsilon)\sin\theta\cos\theta\cos(\pi x)\cos(\pi y)\sin(\pi z)\\ &-\eta\pi\sin(\pi x)\sin(\pi y)\cos(\pi z), \end{aligned}$$

and the boundary condition $g=0$.

Tables 3 and 4 show that the method is almost second order convergence in the sense L_2-norm on uniform meshes and random meshes, respectively. The mesh size and the regularity of the mesh would affect the number of iteration.

https://doi.org/10.4208/cicp.140813.230215a Published online by Cambridge University Press

5.3 Full anisotropic tensor (Robin boundary condition)

Consider the problem (2.3) with Robin boundary condition (2.15). Let

$$\kappa=\begin{pmatrix} a & c & 0\\ c & b & 0\\ 0 & 0 & d\end{pmatrix}=\begin{pmatrix} \cos\theta & -\sin\theta & 0\\ \sin\theta & \cos\theta & 0\\ 0 & 0 & 1\end{pmatrix}\begin{pmatrix} 1 & 0 & 0\\ 0 & \varepsilon & 0\\ 0 & 0 & 1\end{pmatrix}\begin{pmatrix} \cos\theta & \sin\theta & 0\\ -\sin\theta & \cos\theta & 0\\ 0 & 0 & 1\end{pmatrix}.$$

The exact solution is $u=e^{xy}+z^2$. The boundary condition is (2.15) with $\alpha=1.0$, $\beta=1.0$, and

$$\begin{cases} f=-(bx^2+ay^2+2c(1+xy))e^{xy}-2, & \text{in } \Omega,\\ g=(cx+ay+1)e^{xy}+z^2, & \text{on } \partial\Omega_E,\\ g=(bx+cy+1)e^{xy}+z^2, & \text{on } \partial\Omega_N,\\ g=e^{xy}+z^2+2z, & \text{on } \partial\Omega_T,\\ g=(-cx-ay+1)e^{xy}+z^2, & \text{on } \partial\Omega_W,\\ g=(-bx-cy+1)e^{xy}+z^2, & \text{on } \partial\Omega_S,\\ g=e^{xy}+z^2-2z, & \text{on } \partial\Omega_B, \end{cases} \tag{5.1}$$

where $\Omega=[0,1]^3$, $\theta=\frac{\pi}{6}$, $\varepsilon=0.1$ and $\partial\Omega_E=\partial\Omega\cap[x=1]$, $\partial\Omega_N=\partial\Omega\cap[y=1]$, $\partial\Omega_T=\partial\Omega\cap[z=1]$, $\partial\Omega_W=\partial\Omega\cap[x=0]$, $\partial\Omega_S=\partial\Omega\cap[y=0]$, $\partial\Omega_B=\partial\Omega\cap[z=0]$.

Tables 5 and 6 show the convergent results for this problem on uniform and random tetrahedral meshes, respectively. From these tables, one can know that the convergent rate in L_2-norm is almost second order on uniform and random tetrahedral meshes.

Table 5: Numerical results for full anisotropic tensor on uniform tetrahedral meshes.

The number of cell	24×4^3	24×8^3	24×16^3	24×32^3	24×64^3
Mesh size (h)	1/4	1/8	1/16	1/32	1/64
ε_2^u	1.74e-2	4.32e-3	1.07e-3	2.65e-4	6.50e-5
Rate	·····	2.01	2.01	2.02	2.03
The number of iteration	20	22	23	24	24

Table 6: Numerical results for full anisotropic tensor on distorted tetrahedral meshes.

The number of cell	24×4^3	24×8^3	24×16^3	24×32^3	24×64^3
Mesh size (h)	1/4	1/8	1/16	1/32	1/64
ε_2^u	1.83e-2	5.14e-3	1.24e-3	3.25e-4	8.24e-5
Rate	·····	1.83	2.05	1.93	1.98
The number of iteration	20	21	23	25	24

https://doi.org/10.4208/cicp.140813.230215a Published online by Cambridge University Press

5.4 Discontinuous coefficient problem with Dirichlet boundary condition (κ is a scalar)

Consider a discontinuous coefficient problem. The conductivity λ is discontinuous scalar and given by

$$\lambda = \begin{cases} 5.0, & x \leq \frac{1}{2}, \\ 1.0, & x > \frac{1}{2}. \end{cases}$$

The exact solution is

$$u(x,y) = \begin{cases} \sin(\pi x)\sin(\pi y)\sin(\pi z), & x \leq \frac{1}{2}, \\ \sin(5\pi x)\sin(\pi y)\sin(\pi z), & x > \frac{1}{2}. \end{cases}$$

And the corresponding source f is:

$$f(x,y,z) = \begin{cases} 15\sin(\pi x)\sin(\pi y)\sin(\pi z), & x \leq \frac{1}{2}, \\ 27\sin(5\pi x)\sin(\pi y)\sin(\pi z), & x > \frac{1}{2}. \end{cases}$$

This solution and its normal component of flux are continuous at $x = \frac{1}{2}$. As shown in Fig. 5, the numerical results are presented in Table 7. From this table, one can know that our method obtains the second-order convergence rate for the solution on random tetrahedral meshes.

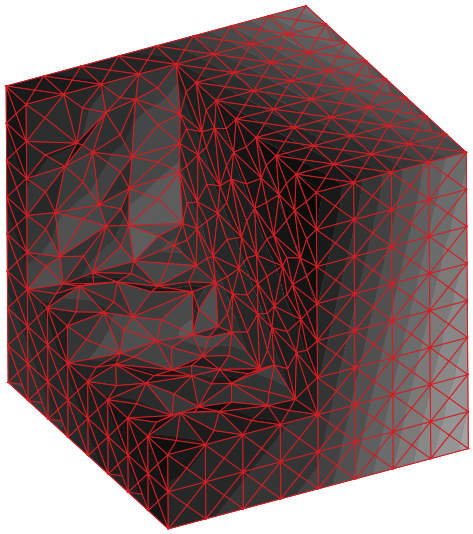


Figure 5: The random tetrahedral meshes with a discontinuity at $x = 0.5(8*8*8)$.

https://doi.org/10.4208/cicp.140813.230215a Published online by Cambridge University Press

Table 7: Numerical results for discontinuous scalar coefficient problem on distorted tetrahedral meshes.

The number of cell	24×4^3	24×8^3	24×16^3	24×32^3	24×64^3
Mesh size (h)	1/4	1/8	1/16	1/32	1/64
ε_2^u	6.96e-3	1.63e-3	4.09e-4	1.01e-4	2.54e-5
Rate	·····	2.09	1.99	2.02	1.99
The number of iteration	18	20	21	21	21

5.5 Discontinuous coefficient problem with Dirichlet boundary condition (κ is a tensor)

Consider a problem with the conductivity κ is discontinuous tensor and given by

$$\kappa=\begin{pmatrix}1&0&0\\0&1&0\\0&0&1\end{pmatrix},\quad x\leq\frac{1}{2},$$
$$\kappa=\begin{pmatrix}2&1&0\\1&2&0\\0&0&1\end{pmatrix},\quad x>\frac{1}{2}.$$

The exact solution is

$$u(x,y)=\begin{cases}(x-0.5)(2\sin(y)+\cos(z))+\sin(y)+z, & x\leq\frac{1}{2},\\ e^{(x-0.5)}\sin(y)+z, & x>\frac{1}{2}.\end{cases}$$

And the corresponding source f is:

$$f(x,y,z)=\begin{cases}(x-0.5)(2\sin(y)+\cos(z))+\sin(y), & x\leq\frac{1}{2},\\ -2e^{(x-0.5)}\cos(y), & x>\frac{1}{2}.\end{cases}$$

This solution and its normal component of flux are continuous at $x=\frac{1}{2}$.

From Table 8, one can know that the convergent rate in L_2-norm is almost second order on random tetrahedral meshes.

Table 8: Numerical results for discontinuous tensor coefficient problem on distorted tetrahedral meshes.

The number of cell	24×4^3	24×8^3	24×16^3	24×32^3	24×64^3
Mesh size (h)	1/4	1/8	1/16	1/32	1/64
ε_2^u	9.33e-4	2.71e-4	7.26e-5	1.92e-5	4.93e-6
Rate	·····	1.78	1.90	1.92	1.96
The number of iteration	16	18	20	19	23

https://doi.org/10.4208/cicp.140813.230215a Published online by Cambridge University Press

6 Conclusion

In this paper we present a new finite volume scheme for three-dimensional diffusion equation on distorted tetrahedral meshes. The resulting scheme offers an explicit expression for the face-centered normal flux, i.e., the discrete normal flux is intuitively a linear combination of the directional flux along the line connecting cell-centers and the tangent flux along the cell-faces. In addition, the vertex unknowns are auxiliary unknowns whose values are solved by a new method, which is presented to eliminate the vertex unknowns for three-dimensional problem, and it does not need to solve local linear systems, so the computation cost is greatly reduced. Although the construction of our scheme is described only on distorted tetrahedral meshes, it is straightforward to extend it to arbitrary polyhedral meshes. Moreover the stability and convergence of the scheme are proved. Numerical results show that the scheme has approximate second-order accuracy in L_2-norm for solution. And from Tables 1 to 8, we can see that the regularity of the mesh, the property of diffusion coefficients and the mesh size would affect the number of iteration.

Acknowledgments

This work is partially supported by NSAF (No. U1430101), the Basic Research Project of National Defense (B1520110011), the National Natural Science Foundation of China (11171036, 91330106), China Postdoctoral Science Foundation (20110490328), the Natural Science Foundation of Shandong Province (ZR2012AM019, ZR2013AM023, ZR2014AM013), the foundation of CAEP (2015B0202042), and Independent Innovation Foundation of Shandong University (2012TS018).

References

[1] D. Li, H. Shui and M. Tang, On the finite difference scheme of two-dimensional parabolic equation on non-rectangular mesh, J. Numer. Methods Comput. Appl., 1 (1980), pp. 217-224.
[2] W. Huang and A. M. Kappen, A study of cell-center finite volume methods for diffusion equations, Mathematics Research Report, 98-10-01, University of Kansas, Lawrence KS66045.
[3] F. Hermeline, A finite volume method for the approximation of diffusion operators on distorted meshes, J. Comput. Phys., 160 (2000), pp. 481-499.
[4] F. Hermeline, Approximation of diffusion operators with discontinuous tensor coefficients on distorted meshes, Comput. Methods Appl. Mech. Eng., 192 (2003) 1939-1959.
[5] G. Yuan and Z. Sheng, Analysis of accuracy of a finite volume scheme for diffusion equations on distorted meshes, J. Comput. Phys., 224 (2007), pp. 1170-1189.
[6] J. E. Morel, J. E. Dendy, M. L. Hall and S. W. White, A cell centered Lagrangian-mesh diffusion differencing scheme, J. Comput. Phys., 103 (1992) 286-299.
[7] M. Shashkov and S. Steinberg, Support-operator finite-difference algorithms for general elliptic problems, J. Comput. Phys., 118 (1995) 131-151.

https://doi.org/10.4208/cicp.140813.230215a Published online by Cambridge University Press

[8] M. Shashkov and S. Steinberg, Solving diffusion equations with rough coefficients in rough grid, J. Comput. Phys., 129 (1996) 383-405.
[9] J. Hyman, M. Shashkov and S. Steinberg, The numerical solution of diffusion problems in strongly heterogeneous non-isotropic material, J. Comput. Phys., 132 (1997) 130-148.
[10] I. Aavatsmark, An introduction to multipoint flux approxmations for quadrilateral grids, Comput. Geosci., 6 (2002), 405-432.
[11] I. Aavatsmark, T. Barkve, O. Boe, T. Mannseth, Discretization on unstructured grids for inhomogeneous, anisotropic media Part I: Derivation of the methods, SIAM J. Sci. Comput., 19 (1998) 1700-1716.
[12] I. Aavatsmark, T. Barkve, O. Boe, T. Mannseth, Discretization on unstructured grids for inhomogeneous, anisotropic media Part II: Discussion and numerical results, SIAM J. Sci. Comput., 19 (1998) 1717-1736.
[13] G. Chen, D. Li, Z. Wan, Difference scheme based on variation principle for two dimensional heat conduction equation, Chinese Journal of Computational Physics, 19 (2002) 299-304.
[14] Z. Sheng and G. Yuan, A nine point scheme for the approximation of diffusion operators on distorted quadrilateral meshes, SIAM J. Sci. Comput., 30 (2008) 1341-1361.
[15] G. Yuan and Z. Sheng, Calculating the vertex unknowns of nine point scheme on quadrilateral meshes for diffusion equation, Science in China Series A: Mathematics, 51 (2008) 1522-1536.
[16] M. G. Edwards and H. Zheng, A quasi-positive family of continuous Darcy-flux finite-volume schemes with full pressure support, J. Comput. Phys., 227 (2008) 9333-9364.
[17] H. A. Friis and M. G. Edwards, A family of MPFA finite-volume schemes with full pressure support for the general tensor pressure equation on cell-centered triangular grids, J. Comput. Phys., 230 (2011) 205-231.
[18] K. Lipnikov, M. Shashkov and I. Yotov, Local flux mimetic finite difference methods, Technical Report LA-UR-05-8364, Los Alamos National Laboratory, 2005.
[19] K. Lipnikov, J. Morel, M. Shashkov, Mimetic finite difference methods for diffusion equations on non-orthogonal non-conformal meshes,J. Comp. Phys. 199 (2004) 589-597.
[20] G. Chen, D. Li, Z. Wan, Difference scheme by integral interpolation method for three dimensional diffusion equation, Chinese Journal of Computational Physics, 20 (2003), 205-209.
[21] Z. Du, D. Yin, X. Liu, J. Lu, Nonorthogonal hexahedralmesh finite volume difference method for the 3-D diffusion equation, J. Tsinghua Univ (Sci & Tech), 43 (2003) 1365-1368.
[22] D. Yin, Z. Du, J. Lu, An unstructured tetrahedral mesh finite volume difference method for the diffusion equation, J. Numer. Methods Comput. Appl., 2 (2005) 92-100.
[23] Y. Coudière, C. Pierre, O. Rousseau, and R. Turpault. A 2d/3d discrete duality finite volume scheme. Application to ecg simulation, Int. Journal on Finite Volumes, (2009), 6(1).
[24] Y. Coudière, F. Hubert, A 3d discrete duality finite volume method for nonlinear elliptic equation. HAL Preprint URL http://bal.archives-ouvertes.fr/docs/00/45/68/37/PDF/ddfv3d.pdf.
[25] Y. Coudière, F. Hubert, G. Manzini, Benchmark 3D:CeVeFE-DDFV, a discrete duality scheme with cell/vertex/face+edge unknowns, J. Fořt et al, Finite volumes for complex applications VI-problems & perspectives, Springer proceedings in mathematics 4, DOI 10.1007/978-3-642-20671-9_95, ©Springer-Verlag Berlin Heidelberg 2011.
[26] F. Hermeline, Approximation of 2-D and 3-D diffusion operators with variable full tensor coefficients on arbitrary meshes, Comput. Method Appl. Mech. Eng., 196 (2007) 2497-2526.
[27] F. Hermeline, em A finite volume method for approximating 3D diffusion operators on general meshes, Journal of Computational Physics, 228 (2009) 5763-5786.

https://doi.org/10.4208/cicp.140813.230215a Published online by Cambridge University Press

[28] M. G. Edwards, H. Zheng, Quasi M-matrix multifamily continuous Darcy-flux approximations with full pressure support on structured and unstructured grids in three dimension, SIAM J. Sci. Comput., 33 (2011) 455-487.
[29] K. Lipnikov, M. Shashkov, D. Svyatskiy, The mimetic finite difference discretization of diffusion problem on unstructured polyhedral meshes, J. Comput. Phys., 211 (2006) 473-491.
[30] J. Wu, Z. Dai, Z. Gao, G. Yuan, Linearity preserving nine-point schemes for diffusion equation on distorted quadrilateral meshes, J. Comput. Phys., 229 (2010) 3382-3401.
[31] M. Bessemoulin-Chatard, C. Chainais-Hillairet and F. Filbet, On discrete functional inequalities for some finite volume schemes, 2012, arXiv:1202.4860v1.
[32] R. Eymard, Th. Gallouet, and R. Herbin, Finite volume methods, In Handbook of numerical analysis, volume VII, 2000, pages 713-1020, North-Holland, Amsterdam.

https://doi.org/10.4208/cicp.140813.230215a Published online by Cambridge University Press